AD-A100 866 MASSACHUSETTS UNIV AMHERST F/G 4/1
A STUDY OF INTERSTELLAR CARBONYL SULFIDE,(U)
SEP 80 P F GOLDSMITH, R A LINKE N00014-76-C-0070
UNCLASSIFIED NL

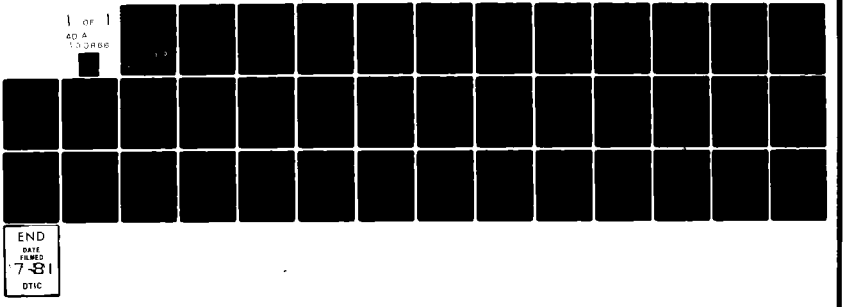

END
DATE FILMED
7-81
DTIC

LEVEL II

(1)

Five College Radio Astronomy Observatory

Reports

Radio Astronomy
GRC TOWER B
University of Massachusetts
Amherst, MA 01003

LEVEL I

(1)

A STUDY OF INTERSTELLAR CARBONYL SULFIDE

Paul F. Goldsmith and Richard A. Linke

#157

DATE: SEPT 23 1980

N00014-69-A-0200-1003

NSF-GP-30424

Accession For	
NTIS GRA&I	X
DTIC TAB	☐
Unannounced	☐
Justification	
By	
Distribution/	
Availability Codes	
Dist	Avail and/or Special
A	

Contract N00014-76-C-0070

Per Ms. Barbara Hughes, ONR, Code 427

A STUDY OF INTERSTELLAR CARBONYL SULFIDE

Paul F. Goldsmith
Five College Radio Astronomy Observatory
University of Massachusetts
Amherst, Massachusetts 01003

Richard A. Linke
Bell Laboratories
Crawford Hill Laboratory
Holmdel, New Jersey 07733

Abstract

We have carried out a study of the carbonyl sulfide (OCS) molecule in 24 interstellar and circumstellar molecular clouds, and detected it in a total of 10 sources and 7 different transitions. Analysis of the data using hydrogen densities derived from a study of CS (Linke and Goldsmith 1980), and assuming that the OCS lines are optically thin, yields a mean column density $\langle N(OCS) \rangle = 3 \times 10^{14}$ cm^{-2} in ten interstellar clouds while the average fractional abundance $\langle N(OCS)/N(H_2) \rangle = 1.6 \times 10^{-9}$, consistent with the theoretical prediction of Oppenheimer and Dalgarno (1974). The results of maps and analysis of multiple transitions in several sources suggest that the regions responsible for the OCS emission are only marginally resolved with a beamsize of ~2'. Direct measurements yield [OCS]/[$O^{13}CS$] = 21 and [OCS]/[$OC^{34}S$] = 16 in SGR B2, compared to terrestrial values of 89 and 23, respectively.

I. INTRODUCTION

Molecules with numerous accessible transitions can contribute to our understanding of interstellar clouds since it is possible for the degree of their excitation to be determined. This information can be most easily obtained if the transitions observed are optically thin, since the complications of radiative transfer are then minimal. Carbonyl sulfide (OCS) is a plausible candidate since it is a simple rotor with rotation constant $2B \simeq 12.16$ GHz, resulting in lines throughout the microwave region. OCS was initially detected in SGR B2 by Jefferts et al. (1971), and several lines from this source were analyzed by Solomon et al. (1973). The line intensities are low, making this type of project difficult but with the very sensitive millimeter wavelength receivers which have recently become available, we have measured several transitions and have made small maps in a number of these lines for four sources: Orion A, SGR A, SGR B2, and W51. In addition, we have obtained detections of one or two lines in seven other sources. In Section II we discuss our OCS data taking procedures and in Section III we analyze the data to determine the OCS abundance and compare the results with theoretical predictions. In Section IV the results of measurements of the rare isotopic species are discussed. An analysis of the intensity of various transitions and maps in Section V provides information about the physical conditions and structure of the central regions of dense interstellar clouds. In Section V we also give results for some of the other molecular transitions detected in the course of this study.

II. DATA

As indicated in Table 1, three different antennas were used to collect the data presented in this paper. For the $J = 2 \rightarrow 1$ observations, a maser preamplifier

was employed on the 37 m Haystack antenna resulting in a system temperature (including sky contribution) of 160 to 300 K, dependent upon elevation and weather conditions. Data were taken by position switching once every ten minutes and spectral resolution obtained with an autocorrelator adjusted for either 16 or 65 kHz resolution depending on source dispersion. A noise tube was used to calibrate the receiver and the standard Haystack efficiency curves provided a calibration of the main beam efficiency which has a maximum of .25 at an elevation of 40 degrees. The beamwidth was determined and the pointing checked by scans of Jupiter. The $J = 4 \rightarrow 3$ data was obtained with the NRAO 36' telescope during a run of CS observations; the calibration procedures are described in detail by Linke and Goldsmith (1980).[1] The higher frequency data taken with cooled mixer receivers

[1]The NRAO is operated by Associated Universities, Inc., under contract with the National Science Foundation.

(Linke, Schneider and Cho 1978) on the BTL 7 m antenna utilized a single sideband calibration system (Goldsmith 1977) which employs liquid nitrogen and ambient temperature absorbers for receiver and atmospheric calibration. The antenna beam efficiencies for these transitions were determined assuming a uniform disc temperature of 170 K for Jupiter and a Gaussian main beamsize derived from scans across the planet. The similarity of the calibration procedures for the lines between 70 and 140 GHz suggests that relative calibrations should be quite accurate; the absolute intensity calibration of these lines is probably accurate to ~20% while that of the lower frequency lines is accurate to ~30%.

The data for OCS of the common isotopic species ($^{16}O^{12}C^{32}S$) is given in Table 2. The antenna temperatures are corrected for atmospheric attenuation and for the beam efficiencies given in Table 1; further details are given in the notes to Table 2. The observations of two different isotopic species are summarized in Table 3. In Figure 1 we present several spectra of the $J = 7 \rightarrow 6$ transition,

which also cover the frequency of the J = 1 → 0 transition of $HC^{18}O^+$. A spectrum of the J = 11 → 10 transition in Orion A is given in Figure 3 and the different spectra obtained in SGR B2 are shown in Figure 4.

III. OCS EXCITATION AND ABUNDANCE

The OCS population is typically distributed over many rotational levels and in order to determine the actual abundance of OCS we must have information about the collision rate, which is the primary determinant of the molecular excitation. Collision rate coefficients for H_2 - OCS have been calculated by Green and Chapman (1978) for temperatures between 10 K and 100 K, including levels up to J = 12. Since over half the population of OCS molecules can be in J > 12 under conditions of interest in molecular clouds, we have included levels up to J = 24, which results in negligible errors for kinetic temperatures $\leq$ 80 K. The deexcitation rate coefficients for higher J were calculated by linear extrapolation of those given by Green and Chapman, and the excitation rate coefficients were obtained by detailed balance. The rates for temperatures between 15 K and 75 K are found to differ from those for 40 K by less than 5% with the exception of several rates pertaining to large ΔJ transitions (in these cases, however, the rates are not of significant magnitudes). We have thus used the deexcitation rate coefficients for 40 K for all kinetic temperatures considered in the analysis of our data. In Figure 2 we give the results of a 25-level calculation. We present the cloud brightness temperature (the antenna temperature detected by a lossless antenna above the atmosphere with the source filling the beam) versus the quantum number of the OCS transition; the different curves are parameterized by molecular hydrogen density and kinetic temperature. The OCS abundance is fixed in terms of fractional abundance [$X(OCS) = n(OCS)/n(H_2)$] per unit velocity gradient, which, when multiplied by hydrogen density, is equivalent to OCS abundance per unit linewidth.

The predicted antenna temperatures vs. J follow smooth patterns; this behavior persists despite population inversions in the J = 2 → 1 and J = 1 → 0 transitions for $n(H_2) \leq 3 \times 10^3$ cm^{-3} which result from the rapid decrease of the A-coefficients as one approaches the bottom of the rotational ladder (Goldsmith 1972). The predicted optical depths are very small, however, and the antenna temperatures hence do not reflect any amplification. The observed intensities of the various transitions discussed in Section V do not imply the presence of any significant exponential gain in the J = 2 → 1 transition; the linewidths in the two sources in which this line was detected are not anomalous compared to the widths of the other transitions.

For the sources in which we have observed only a single OCS transition, we cannot determine the hydrogen density and so we have used the densities derived by Linke and Goldsmith (1980) from a study of CS. Hydrogen densities derived from OCS are discussed in §V below. The cloud temperatures are also taken from Linke and Goldsmith except where indicated. Since the OCS excitation is not very sensitive to the kinetic temperature, the relatively coarse quantization used does not introduce a significant error. For a Gaussian lineshape and assuming uniform excitation across the line profile, one determines that

$$N(OCS)(cm^{-2}) = 3.3 \times 10^{18} \left|\frac{X(OCS)}{dv/dr}\right| n(H_2)\ \Delta V_{FWHM} \qquad (1)$$

with dv/dr in km s^{-1} pc^{-1} and ΔV_{FWHM} in km s^{-1}. The derived OCS column densities (or upper limits) are given in Table 4.

The OCS column densities can be compared to those of CS; from the sources analyzed by Linke and Goldsmith (1980) there are nine with detections of both molecules. For these, a cross correlation analysis of the column densities yields $N(OCS) \propto N(CS)^{1.6}$ with a correlation coefficient of .90. The mean ratio of column densities is $\langle N(OCS)/N(CS) \rangle = .22$. It is possible, however, that the CS abundance

estimates are too low due to problems with uncorrected saturation (Frerking et al. 1980). If we use the CS abundance suggested by Frerking et al. for six sources in common, we obtain $N(OCS) \propto N(CS)^{.91}$ with a correlation coefficient of .95. It thus appears that we can only restrict the column density relationship to lie within these limits. The mean value of N(OCS)/N(CS) for these six sources is .02, after this correction has been applied. The majority of non-detections of OCS are probably the result of inadequate sensitivity and sources with moderate column density; there are however three sources, DR21(OH), M17, and NGC 6334, which appear to be deficient in OCS when compared to the sample as a whole. The most striking example is DR21(OH) for which our non-detection places a (1 σ) upper limit on the OCS abundance a factor of 11 below that expected from the abundance of CS (as this source was not observed by Frerking et al. we have no information on the possible uncorrected CS saturation in this source). The study of Wootten et al. (1978) indicates that the fractional abundance of a number of species in this region is somewhat low; the CS fractional abundance is found to be close to the average for giant molecular clouds (Linke and Goldsmith 1980). There thus appears to be an abundance anomaly for OCS in this source.

In order to compare the OCS abundance with that predicted from chemical theories, it is useful to know the volume density of OCS or the fractional abundance itself. This requires that the source size be known and, as discussed in Section V, the sources are barely, if at all, resolved by the antennas we have used (except for one dimension in SGR B2). Using source sizes derived by deconvolving our maps assuming Gaussian intensity distributions for the emitting regions, we obtain the OCS fractional abundances given in Table 5 which may be viewed as lower limits. These values fall within the range 8×10^{-11} to 2×10^{-8} suggested by Oppenheimer and Dalgarno (1974), who propose that the major pathway for formation of OCS is $S^- + CO \rightarrow OCS + e^-$. There does not appear to be any

significant correlation of OCS abundance with source kinetic temperature.[2]

[2]This result is obtained by noting that (1) in the sample of sources for which X(CS) was determined by Linke and Goldsmith (1980) there is no significant correlation of kinetic temperature and abundance, and (2) the ratio N(OCS)/N(CS) also shows no correlation with the source temperature. The modifications of N(CS) suggested by Frerking et al. (1980) do not alter this conclusion.

This result indicates that the additional source of OCS at low temperatures postulated by Prasad and Huntress (1980) is not required.

The OCS linewidths are quite similar to those of CS but tend to be somewhat narrower; in Orion A and W51, the two sources for which we have maps in both species, the CS source size is 2-4 times larger than that for OCS.[3]

[3]In the case of Orion A, we consider only source size in RA to avoid confusion due to the beam-diluted, very narrow N-S ridge source discussed by Goldsmith et al. (1980).

Since it is unlikely that excitation effects would produce this result, it appears that the OCS is restricted to the small central regions of very high molecular hydrogen density.

IV. ISOTOPIC ABUNDANCE RATIOS

The observational data on two rare isotopic species of OCS are given in Table 3. Analysis of the abundance ratios is relatively straightfoward since these extremely weak lines are very likely to be optically thin.[4] The data for the

[4]Since the $O^{13}CS$ line frequencies differ from those of OCS by less than 1 percent, effects resulting from the excitation of species with different level spacings

(Linke et al. 1977) are negligible. In the case of $OC^{34}S$ the frequency is 2.5 percent lower than that of OCS (the frequencies are given in Table 3). In the limit of complete thermalization at a kinetic temperature of 20 K, as is suggested by the results of Section V, we find a difference of only 1 percent in the constants relating antenna temperature and column density for the two species. An additional correction is required if the source does not fill the antenna beam; in the limit of a completely unresolved source observed with the same diffraction-limited antenna the constant relating antenna temperature and molecular abundance will contain an additional factor ν^2, compared to the situation when the beam is filled by a uniform source. Strictly speaking, this applies to an antenna whose beamwidth is proportional to the wavelength; frequency-independent illumination and losses are thus also assumed. These criteria are met by the Crawford Hill 7-m antenna, and approximately satisfied when data from the other antennas used is analyzed in the manner described in Section II. The maps of SGR B2 suggest that the region with observable OCS emission, while somewhat extended compared to our beam, is strongly centrally condensed. Hence the true correction for the source size is not as great as ν^2 and its effect, an increase in the abundance ratio $[O^{34}CS]/[OCS]$ by ~2 percent compared to $T_A^*(O^{34}CS)/T_A^*(OCS)$, is negligible.

---

7 → 6 transition from Table 3 yield $[O^{13}CS]/OC^{34}S] = 0.80 \pm 0.32$. We can also use the 9 → 8 $OC^{34}S$ line and the 8 → 7 $O^{13}CS$ line by making a correction for the different transitions involved, which yields $[O^{13}CS]/[OC^{34}S] = 0.75 \pm 0.25$. The weighted average double ratio is 0.77 ± 0.20 (1 σ).[5] This is to be compared with

---

[5]The errors include the uncertainties in the measurements of the line intensities but not in the corrections; the latter probably do not exceed 15%.

the terrestrial double ratio $([^{13}C]/[^{12}C])/([^{32}S]/[^{34}S]) = 0.26$, and the value for SGR B2 $[^{13}CS]/[C^{34}S] = 0.66$ given by Frerking et al. (1980). Our result is clearly value. The OCS isotopic lines are approximately a factor of ten weaker than those of CS with corresponding less likelihood of saturation: the close agreement between these two molecules in SGR B2 suggests that we are correctly determining the double isotopic ratio in this source.

Since we have measured the OCS line as well as those of the rarer isotopes, we can attempt to derive the single isotopic abundance ratios individually. The major question in this procedure is whether the OCS lines are optically thin; while the weakness of the line, 1 K, compared to the kinetic temperature of 20 K derived from CO (Scoville, Solomon, and Penzias 1975) might suggest that the line is optically thin, or at least in the linear regime in which the antenna temperature is proportional to abundance, irrespective of τ (Linke et al. 1977), the complex temperature and density structure of the gas in the direction of SGR B2 suggests careful examination of this assumption. We do see a marginally significant (1 σ, see Table 3) systematic increase in the relative strength of the rare isotopes as we go to higher transitions, which have larger antenna temperatures. However, the relative opacities of the various transitions obtained from the source modeling (see IVc below) cannot explain the dependence of the observed isotopic ratio on the transition observed in terms of differential saturation of the OCS transitions. Since the pairs of measurements of each ratio are consistent to within the 1 σ combined errors, we can derive weighted mean ratios $O^{12}CS / O^{13}CS = 21.1 \pm 4.9$[6]

[6]This value for the carbon isotopic ratio agrees with that of 22 ± 1 determined by Wannier and Linke (1978) and is likely to suffer less from any saturation effects due to the weaker lines measured here; it is also consistent with the value 24 ± 3 (1 σ) determined by Lazareff, Lucas, and Encrenaz (1978) from observations of formamide (NH$_2$CHO).

and $[OCS]/[OC^{34}S] = 15.8 \pm 2.2$. The possible role of chemical fractionation is difficult to assess in this complex source but in view of its fairly high temperature, this is not likely to be an important effect. At the present time, it therefore appears that the sulfur, as well as the carbon, isotopic ratios in SGR B2 are distinctly non-terrestrial.

V. MULTIPLE TRANSITION OBSERVATIONS AND CLOUD STRUCTURE

Two significant obstacles to the accurate determinat of conditions within molecular clouds are the proper assessment of source dimensions when data is taken with beams of different size, and the extent of variations along the line-of-sight. These problems both play a significant role in analysis of the OCS observations. The four sources, Orion A, SGR A, SGR B2, and W51 are discussed individually below.

a) Orion A

The results of maps in two different frequencies suggest that the OCS emitting region has a FWHM size of ~1' in RA by 1!2 - 1!5 in DEC, assuming a Gaussian source intensity distribution. Since these results are obtained by deconvolving maps made with beam sizes 2!5 to 1!6 (see Table 1), we must be somewhat suspicious of their accuracy, but there is no doubt that the OCS emitting region is very small. This has a significant impact on the analysis of our data due to the different beamsizes we employed. The uncorrected intensities of the six transitions we have detected do not fall in a pattern resembling any of the curves in Figure 2; however, if we assume that the source is essentially unresolved at all of the frequencies we have used, and correct each intensity by a relative factor $(\theta_{FWHM}\ (\text{antenna}))^2$ much better agreement is obtained. The result is that the data fits the curves for $n_{H_2} = 10^5$

or 10^6 cm^{-3} with $T_{KINETIC}$ = 75 K; since the curves for $n_{H_2} > 10^5$ cm^{-3} merge together for the range of transitions we have observed, we can only set $n_{H_2} = 10^5$ cm^{-3} as a lower limit to the molecular hydrogen density. The actual OCS fractional abundance will depend on the source size. Since the source does not appear vastly smaller than the beamsizes we have used, the uncertainty in hydrogen density remains the dominant uncertainty in determining the fractional abundance which could, however, be somewhat higher than that given in Table 5.

Emission with high velocity dispersion is visible in the J = 9 → 8 and J = 11 → 10 OCS spectra taken at the central position of Orion A; the latter is shown in Figure 3. This component has a linewidth of ~ 15 km s^{-1} and a peak temperature of 25 percent of the narrow emission in both transitions. Its central velocity is 5 km s^{-1}. The shape of this feature is very similar to that of HC^{15}N (Linke et al. 1977), narrower than the broad HC_3N emission feature (Wannier and Linke 1978) but somewhat wider than the intermediate width ammonia component (Morris, Palmer, and Zuckerman 1980). It is thus not entirely clear whether to identify this emission with the "CO plateau" feature (Zuckerman, Kuiper, and Kuiper 1976) or the "hot core" component discussed by Morris, Palmer, and Zuckerman 1980. Taking T = 210 K, $n(H_2) = 10^6$ cm^{-3} (Goldsmith et al. 1980), and source diameter 30" (Solomon, Scoville, and Huguenin 1980) for the plateau characteristics, we find that X(OCS) is 6 x 10^{-8} in this region; an increase of a factor of 15 above the narrow-dispersion Orion A cloud. Taking T = 250 K, $n(H_2) = 5 \times 10^7$ and D = 6" for the characteristics of the hot core region (Morris, Palmer, and Zuckerman 1980) we find that the OCS fractional abundance is 3 x 10^{-7}. Lada, Oppenheimer, and Hartquist (1978) and Hartquist, Oppenheimer, and Dalgarno (1980) have considered the effect of the passage of a shock on the OCS abundance, and conclude that as a result of the reactions $H_2 + S \rightarrow HS + H$ and $HS + CO \rightarrow OCS + H$, X(OCS) may approach 10^{-7} behind the shock. This value is

in quite good agreement with our determination, and suggests that whichever region is responsible for the OCS high dispersion emission has been affected by the passage of a shock.

Our observations of high dispersion emission centered at $V_{LSR} \sim 5$ km s^{-1} in two transitions confirms that this emission is produced by OCS in the respective rotational transitions also responsible for the narrow emission features; the possibility suggested by Lada, Oppenheimer, and Hartquist (1978) of emission from an unknown molecule in their image sideband being responsible for the broad emission associated with OCS J = 8 → 7 appears unlikely. With our relatively large beamsize it is difficult to determine the center of the high dispersion emission; there is a suggestion of a broad feature with $T_A^* \sim .1$ K at the (0,1) position when observed in the 11 → 10 OCS transition, but this is no more than half the strength of the high dispersion emission at the (0,0) position (Figure 1). There is no suggestion of high dispersion emission at the (0,-1) position and we thus have weak evidence for a modest ($\lesssim$30") northward displacement of the high velocity dispersion gas with respect to KL.

b) SGR A

The J = 7 → 6 mapping data shows a source only marginally resolved in DEC (FWHM ~3') but close to unresolved in RA. If the effects of one dimensional dilution are removed from the line intensities, we can obtain a good fit for the three transitions observed for hydrogen densities between 10^4 cm^{-3} and 3×10^4 cm^{-3}. The fit for either two-dimensional dilution or no dilution is quite poor.

c) SGR B2

We have observed 7 OCS transitions in SGR B2; their intensities given in Table 2 are nearly equal which is not a characteristic of any of the

excitation curves of Figure 1. The map in the J = 7 → 6 transition indicates that the intensity peaks approximately 2' north of our central (OH maser) position and that the source is extended ($\Delta\theta \sim 4'$ FWHM) in DEC. An extension to the north of the OH maser position is also seen in the contours of $\tau(H_2CO\ 2\ cm)$ and $N(^{13}CO)$ (Scoville, Solomon, and Penzias 1975). The OCS source size in RA is small ($\lesssim 2'$) and thus we probably have to deal with some beam dilution effects. Scaling our data in proportion to θ_{FWHM} (antenna) as would be appropriate for a source unresolved in one dimension, we obtain a curve in good agreement with that for n_{H_2} between 10^4 cm^{-3} and 10^5 cm^{-3}, which agrees well with the density determined from CS by Linke and Goldsmith (1980) and Frerking et al. (1980). The presence of beam dilution is given further support by the ratios of intensities of different transitions of the isotopic species $O^{13}CS$ and $OC^{34}S$ (see Table 3). These intensities increase somewhat faster than the maximum rate ν^2 allowed for optically thin lines from a resolved source.

It was noted some time ago that many spectral lines observed in SGR B2 show doubly peaked profiles, which are most reasonably attributed to self (or foreground) absorption (Scoville, Solomon, and Penzias 1975, hereafter SSP). Both CS J = 2 → 1 and J = 1 → 0 share this characteristic (Linke and Goldsmith 1980) as does to a remarkable extent $H^{13}CN$ (Linke et al. 1977, hereafter LGWWP). Lines of less abundant species are often single-peaked--including ^{13}CS and $C^{34}S$ (Frerking et al. 1980), $HC^{15}N$ (LGWWP), HC_3N and its ^{13}C-substituted variants (Wannier and Linke 1978) as well as OCS and its isotopically substituted species. There does not appear to be any correlation between absolute line strength and the "self-absorbed" appearance--the $H^{13}CN$ line has T_A^* (max) of only .7 K but drops to less than 10 percent of this value at V ~ 60 km s^{-1}, while the HC_3N J = 9 → 8 line which has $T_A^*(max) \simeq 2.5$ K shows no suggestion of self-reversal. This behavior can be attributed, as suggested in SSP, to a difference in the excitation conditions relevant to the foreground

absorbing material compared with the "core" emission source. If the foreground material has a lower density then the high lying levels [e.g. HC_3N (9 → 8)] will have no appreciable population and will not therefore present any opacity to the emission from the core. On the other hand, ground states of HCN, HCO^+ and CS, for example, will be relatively highly populated and will present high opacity at a at a low excitation temperature and thus produce the self-reversal.[7]

[7] If the emission of such species as $H^{13}CN$ is being greatly affected by foreground absorption, the intrinsic linewidth of the background cloud may be far lower than that obtained from the FWHM of the actual line profile. This will tend to partially cancel the error made by neglecting the absorption when determining the column density.

A number of studies have suggested that the density structure along the line-of-sight to SGR B2 is complex. In addition to the study by SSP, a study of HC_3N emission by Morris et al. (1976), hereafter MTPZ, suggests a core-halo model with $n_{H_2} = 10^6$ cm^{-3} in a core of angular diameter 2'.4 and $n_{H_2} = 10^4$ cm^{-3} in the lower-density region having an angular diameter of 5'. A three-component model has been proposed by Avery et al. 1979 to explain their observations of HC_5N in a manner consistent with MTPZ: they suggest an inner region 2'.4 in diameter having $n(H_2) = 10^6$ cm^{-3}, a middle region 5' in diameter with density 3000 cm^{-3}, and an envelope 10' in diameter having $n(H_2) = 10^2$ cm^{-3}. Our OCS results indicate a density less than that suggested by these authors for the core region and a source size somewhat greater. The present, as well as other density determinations, must be viewed with some caution particularly due to possible problems of saturation. The reasonable fit of the intensities we have measured to a single molecular hydrogen density does not imply that the density throughout the cloud is uniform. We feel that the OCS data are consistent with a strongly centrally condensed

hydrogen density distribution; since the excitation of the OCS lines we have observed is not sensitive to hydrogen densities >> 10^5 cm^{-3}, we cannot rule out the presence of a very small high density source as suggested by the observations of CH_3CN by Solomon et al. (1971).

d) W51

This source gives convincing evidence for the very small angular size of its OCS-emitting region. The map in the J = 11 → 10 line suggests that the peak of the source may be displaced by ~0!5 in RA from our (0,0) position and that the source is slightly extended in this coordinate, but is extremely small (FWHM < 1!1) in DEC. A second indication that we are seeing substantial beam dilution is the ratios of the antenna temperatures of successive transitions. Both the ratios $T_A(8 \rightarrow 7)/T_A(7 \rightarrow 6)$ and $T_A(9 \rightarrow 8)/T_A(8 \rightarrow 7)$ exceed the resolved source limit and hence are indications that the emission is dominated by an unresolved region.[8] The molecular hydrogen density indicated is between ≈ 10^4 and 10^5 cm^{-3}, consistent with the 10^5 cm^{-3} determined by Linke and Goldsmith (1980).

[8] The (8 → 7)/(7 → 6) ratio even exceeds the unresolved source limit by about 30%, but taking the 1 σ errors in the proper sense just brings the ratio into agreement with the unresolved source limit.

e) Other Sources

For NGC 2264 we have detected two OCS transitions but without any mapping data we cannot accurately assess beam dilution effects. If following the results obtained for the other clouds, we assume an unresolved source, the relative antenna temperatures constrain the hydrogen density to lie between 10^4 and 6 x 10^4 cm^{-3}.

f) Other Molecular Lines

$\underline{HC^{18}O^+}$: The J = 1 → 0 line of $HC^{18}O^+$ has been detected in six sources; its frequency is only 23 MHz higher than that of the J = 7 → 6 line of OCS. Some of the data presented here were obtained as part of a study of $HC^{18}O^+$ (Stark 1980). The intensities and derived abundances are given in Table 6. The molecular hydrogen densities have again been taken from Linke and Goldsmith (1980); the $HC^{18}O^+$ linewidths have been used to derive the column densities except for Orion A and W51 where due to the low $HC^{18}O^+$ signal-to-noise ratio we have used the OCS linewidth which is very close to that of the $HC^{18}O^+$ in the sources in which both molecules have been detected. It is obvious from the data presented in Table 6 that there are large variations in the relative abundances of $HC^{18}O^+$ and OCS. DR21(OH) is again prominent due to the lack of observed OCS and the correspondingly large lower limit on $N(HC^{18}O^+)/N(OCS)$, which is over two orders of magnitude larger than the measured ratio in Orion A. The large relative abundance variations suggest that care must be exercised in the application of any chemical modeling scheme to a particular molecular cloud.

$\underline{HC_5N}$: In Figure 5 we present a spectrum taken in an attempt to detect the J = 7 → 6 OCS line in the infrared source IRC + 10216. Molecular lines in this source characteristically are found to have V_{LSR} = -26 km s^{-1} (Morris et al. 1976, Kuiper et al. 1976); we did not detect OCS emission in either this transition or in the J = 2 → 1 line (see Table 2 for limits). The J = 7 → 6 spectrum clearly contains a line with rest frequency ν_o = 85201 ± 1 MHz, assuming V_{LSR} = 26 km s^{-1}. This frequency is within 1.4 MHz of the frequency 85202.4 MHz predicted for the J = 32 → 31 transition of HC_5N, based on the rotational constant B_o = 1331.331 MHz given by Avery et al. (1979) and the centrifugal stretching constant derived from the frequency for the J = 9 → 8 line given by Winnewisser and Walmsley (1978). The linewidth is 27.5 km s^{-1} FWHM and the peak T_A^* = .036 ± .008 K. The source diameter

of 40-60" obtained for the J = 9 → 8 HC_5N line indicates that we are suffering from significant beam dilution; taking a source disk diameter of 50" we derive a brightness temperature of .94 K. The 9 → 8 line observed by Winnewisser and Walmsley (1978) has a brightness temperature of 1.4 K. The ratio of these temperatures indicates an excitation temperature of 21 K, which is reasonably consistent with that implied by the data of Morris (1975) for the 12 → 11 and 5 → 4 transitions of HC_3N which have A-coefficients similar to those of the pair of HC_5N transitions we have observed. This situation should hold if both species are excited by the IR pumping model developed by Morris (1975).

We have also detected this line in SGR B2 ($T_A^* \simeq .15$ K) but not in any other of the sources we have studied.

VI. SUMMARY AND CONCLUSIONS

We have found that in the centers of giant molecular clouds carbonyl sulfide (OCS) is a moderately common molecule with a mean fractional abundance X(OCS) = $n(OCS)/n(H_2) = 1.6 \times 10^{-9}$. This is similar to the abundance of HCO^+ and approximately 5 times greater than the abundance of HC_3N. The OCS abundance is approximately one tenth of that of CS and the column densities of the two species are highly correlated. Several sources, with DR21(OH) the outstanding example, do appear to be deficient in OCS when compared to the column density expected from CS observations. The abundance of OCS is in good agreement with theoretical predictions based on production from S^- ions. The OCS transitions have low opacity due to the relatively low molecular dipole moment and the relative ease with which a large number of levels are populated. We have observed the rare isotopic species $O^{13}CS$ and $OC^{34}S$ in SGR B2 and, although there is a possibility of some saturation in the lines of the common species, we determine that $[OCS]/[O^{13}CS] = 21 \pm 5$ and $[OCS]/OC^{34}S] = 16 \pm 2$.

The sizes of the OCS emitting regions are, with the exception of one dimension in SGR B2, only marginally resolved with beamsize of ~2'. Since much larger regions with density sufficient to excite the OCS transitions observed are known to exist, we conclude in the context of centrally condensed source models that the OCS fractional abundance increases in regions of higher density. The intensities of the OCS transitions can be satisfactorily fitted by a single molecular hydrogen density after effects of beam dilution are taken into account. The density determined in each source is in good agreement with that determined from the excitation of CS. It appears that the lack of OCS in low density regions and the relative insensitivity of the transitions to densities much greater than 10^5 cm^{-3} allow the wide range of transitions observed (A coefficients between 3×10^{-8} s^{-1} and 7×10^{-6} s^{-1}) to be consistent with a single density, although the sources observed undoubtedly encompass large density variations.

VII. ACKNOWLEDGEMENTS

We are indebted to A.A. Stark for allowing us to combine his $HC^{18}O^+$ data with our data for OCS 7 → 6 in two of our sources. We gratefully acknowledge the assistance of A.C. Cheung, R.L. Plambeck, and W.J. Wilson in initial attempts to begin the study of OCS emission. We wish to thank W.D. Langer for interesting discussions concerning the chemistry of OCS. Mark Morris contributed valuable suggestions for clarification of the discussion. The Five College Radio Astronomy Observatory is operated with support from the National Science Foundation under grant AST 76-24610 and with the permission of the Metropolitan District Commission. This is contribution no. 434 of the Five College Astronomy Department.

TABLE 1

TELESCOPE PARAMETERS FOR OCS OBSERVATIONS

Transition	Frequency (MHz)[a]	Antenna	Beamwidth (min arc)[b]	Main Beam Efficiency
2 → 1	24325.93	Haystack 37 m	1.4	$\leq$.25[c]
4 → 3	48651.64	NRAO 11 m	2.6	.69[d]
6 → 5	72976.80	BTL 7 m	2.9	.95[e]
7 → 6	85139.11	BTL 7 m	2.5	.94
8 → 7	97301.21	BTL 7 m	2.2	.87
9 → 8	109463.06	BTL 7 m	1.9	.79
11 → 10	133785.90	BTL 7 m	1.6	.70

a. Frequencies from Maki 1974.

b. FWHM determined from scans of Jupiter.

c. Standard 22 GHz gain and efficiency curves used.

d. See Linke and Goldsmith 1980 for discussion.

e. All BTL calibrations determined assuming a temperature of 170 K for Jupiter and that the main lobe has a Gaussian shape whose angular size is defined by the measured FWHM beamwidths given above.

TABLE 2

OBSERVATIONS OF OCS

Source									
RA(1950)	DEC(1950)	NAME	Transition	T_A^{*} [a] (K)	σ_T	V_{LSR} (km s^{-1})	σ_V	ΔV (km s^{-1})	$\sigma_{\Delta V}$
02:21:55.0	61:51:59	W3(OH)	9 → 8		[.085]			[.69]	
02:59:22.0	60:16:00	IC1848	7 → 6		[.10]			[.88]	
03:25:56.0	31:10:38	NGC1333	7 → 6		[.018]			[.88]	
			9 → 8		[.028]			[.69]	
04:29:25.0	24:16:54	TAURUS	7 → 6		[.018]			[.88]	
05:32:47.0	-05:24:30	ORION A	2 → 1	.16	.01	7.8	.2	5.9	.5
			6 → 5	.23	.02	8.0	.3	4.3	.8
			7 → 6	.31	.02	8.0	.2	4.3	.4
		(-1,0)		.25	.04	7.8	.5	3.7	1.2
		(0,1)		.22	.03	7.6	.4	4.3	1.1
		(0,-1)		.19	.04	6.7	.6	4.5	1.9
		(0,-2)			[.08]			[.88]	
		(1,0)		.18	.03	8.7	.8	5.5	3.7
			8 → 7	.46	.04	8.1	.2	4.9	.6
			9 → 8	.89	.03	8.1	.1	4.8	.2
		(-1,0)		.48	.06	7.8	.3	3.5	.7
		(0,2)		.18	.04	10.1	3.9	---b	---b
		(0,1)		.38	.05	8.4	.5	5.0	1.2
		(0,-1)		.63	.08	8.2	.2	3.2	.5
		(0,-2)		.27	.05	7.9	2.0	10.6	---b
		(1,0)		.33	.05	7.6	.6	5.3	1.9
			11 → 10	1.49	.10	8.0	.2	4.3	.4
		(-2,0)			[.10]			[.56]	
		(-1,0)		.63	.07	7.8	.4	4.6	1.4
		(0,2)			[.13]			[.56]	
		(0,1)			[.10]			[.56]	
		(0,-1)		.69	.07	7.7	.4	4.5	1.2
		(0,-2)		.29	.06	6.9	.8	5.3	3.0
		(0,-3)			[.11]			[.56]	
		(1,3)			[.11]			[.56]	
		(1,0)		.60	.09	7.9	.3	2.7	.9
		(2,0)			[.10]			[.56]	

Table 2--continued

Source			Transition	T_A^{*} [a] (K)	σ_T	V_{LSR} (km s^{-1})	σ_V	ΔV (km s^{-1})	$\sigma_{\Delta V}$
RA(1950)	DEC(1950)	NAME							
05:39:12.0	-01:55:42	ORION B	7 → 6		[.09]			[.88]	
			9 → 8		[.07]			[.69]	
06:05:22.0	-06:22:35	MON R2	9 → 8	.05	.025	12.0	2.5	5.75	---b
06:10:01.1	-18:00:00	S255	9 → 8		[.08]			.69	
06:38:25.0	09:32:39	NGC2264	2 → 1		[.067]			[.2]	
			7 → 6	.064	.011	8.1	.7	5.1	2.1
			9 → 8	.11	.04	7.5	.6	2.7	1.7
09:46:48:7	13:22:39	IRC+10216	2 → 1		[.013]			.8	
			7 → 6		[.008]			[3.5]	
13:46:12.0	-28:07:06	W HYA	7 → 6		[.04]			[.88]	
15:51:02.0	-04:33:34	L134	7 → 6		[.09]			[.88]	
16:23:35.0	-24:19:00	ρ OPH	2 → 1		[.11]			[.2]	
			7 → 6		[.04]			[.88]	
17:17:33.0	-35:44:00	NGC6334	7 → 6		[.18]			[.88]	
17:42.42	-27:59:00	SGR A	6 → 5	.25	.02	46.1	1.2	23.2	3.1
			7 → 6	.27	.01	47.3	.8	24.1	1.1
		(-2,0)		.10	.02	43.9	6.2	31.7	20.7
		(0,2)		.17	.04	53.1	5.7	31.2	20.7
		(0,-2)		.13	.02	39.5	3.7	35.4	13.5
		(2,0)		.09	.02	45.9	3.7	19.5	12.6
			11 → 10	.46	.04	48.9	2.0	29.9	7.0
17:44:11	-28:22:30	SGR B2	2 → 1	.30	.02	63.1	.6	18.9	1.4
			4 → 3	.88	.09	57.4	1.4	19.3	3.5
			6 → 5	.73	.03	60.5	.8	20.6	2.7
			7 → 6	.86	.01	63.1	.2	22.8	.65
		(-4,0)			[.33]			[.88]	
		(-2,2)		.35	.04	58.0	3.6	39.3	14.3
		(-2,0)		.39	.04	62.7	2.0	25.9	7.3
		(-2,-2)		.26	.05	53.4	3.1	22.1	15.3
		(0,4)		.23	.06	65.4	3.1	16.8	10.0
		(0,2)		.82	.04	64.2	.8	23.6	2.1
		(0,-2)		.45	.03	54.8	1.4	23.6	4.4
		(0,-4)		.35	.05	50.7	1.8	16.0	6.0

Table 2--continued

Source									
RA(1950)	DEC(1950)	NAME	Transition	T_A^* [a] (K)	σ_T	V_{LSR} (km s^{-1})	σ_V	ΔV (km s^{-1})	$\sigma_{\Delta V}$
		(0,-6)			[.10]			[.88]	
		(2,2)		.25	.04	60.2	3.2	26.4	14.1
		(2,0)		.26	.02	60.9	2.7	30.8	14.1
		(2,-2)		.21	.05	58.3	5.2	27.5	20.7
			8 → 7	.95	.07	60.9	1.2	23.8	3.6
			9 → 8	1.24	.08	61.9	.9	20.5	2.7
			11 → 10	1.18	.06	61.4	.6	19.6	1.7
18:11:19.0	-17:56:46	W33	9 → 8	.23	.10	36.6	.8	3.0	2.0
18:17:27.0	-16:14:54	M17L	7 → 6		[.03]			[.88]	
18:17:31.0	-16:12:50	M17A	2 → 1		[.10]			[.2]	
			7 → 6	.04	.02	19.8	2.0	7.4	9.5
18.33.26.0	-07:16:00	K39	7 → 6	.14	.04	20.4	9.2	45.6	43
19:21:27	14:24:30	W51	2 → 1		[.07]			[.2]	
			7 → 6	.06	.01	56.3	3.1	20.9	18.2
			8 → 7	.14	.02	57.2	.9	11.1	2.0
			9 → 8	.23	.01	56.8	.5	10.5	1.3
			11 → 10	.29	.03	56.6	.5	6.8	1.4
		(-1,0)		.29	.04	58.0	.8	8.6	1.5
		(0,1)			[.07]			[.56]	
		(0,-1)		.14	.04	56.1	3.3	12.2	13.2
		(1,0)		.11	.06	56.0	1.1	3.6	2.2
19:34:34.0	07:27:00	B335	7 → 6		[.02]			[.88]	
20:37:14.0	42:12:00	DR21(OH)	2 → 1		[.04]			[.8]	
			7 → 6		[.009]			[.88]	
23:11:37.0	61:12:00	NGC7538	9 → 8	.08	.025	-57.1	1.1	4.5	6.0

a. In the cases where a line was detected all parameters given are the result of a Gaussian fit to the data, σ_T and $\sigma_{\Delta V}$ being the 1 σ uncertainties of the peak temperature and linewidth respectively. The antenna temperatures are corrected for beam efficiency (see Table 1) and atmospheric attenuation to obtain T_A^*. For non-detections we give (enclosed

Table 2--continued

in brackets in the σ_T column) the RMS noise in a channel of width ΔV. Entries in parentheses under source name are offsets in minutes of arc from the central position of the source.

b. Line parameters not meaningful due to low signal-to-noise ratio or baseline problems.

TABLE 3

OCS ISOTOPIC OBSERVATIONS IN SGR B2[a]

Species	Transition[b]	T_A^* (K)	σ_T	V_{LSR} (km s^{-1})	σ_V	ΔV (km s^{-1})	$\sigma_{\Delta V}$
$O^{13}CS$	6 → 5		[.04]			[1.03]	
	7 → 6	.032	.01	57.3	5.7	16.1	40.8
	8 → 7	.069	.02	56.0	3.7	18.5	10.5
$OC^{34}S$	7 → 6	.040	.01	59.0	4.0	27.6	11.0
	9 → 8	.089	.013	64.9	3.8	26.3	16.5

a. The source position is the same as that given in Table 2.

b. The transition frequencies (in GHz) are: $O^{13}CS$ 6 → 5, 72.741977; $O^{13}CS$ 7 → 6, 84.865166; $O^{13}CS$ 8 → 7, 96.988139; $OC^{34}S$ 7 → 6, 83.05799; and $OC^{34}S$ 9 → 8, 106.78738, all from Maki (1974).

TABLE 4

OCS COLUMN DENSITIES AND UPPER LIMITS[a]

Source	N(OCS) (cm^{-2})
W3(OH)	$< 4 \times 10^{13}$
IC 1848	$< 3 \times 10^{13}$
NGC 1333[b]	$< 6 \times 10^{12}$
TMC[c]	$< 3 \times 10^{12}$
ORI A	4×10^{14}
ORI B	$< 2 \times 10^{13}$
MON R2	1×10^{13}
S255	$< 2 \times 10^{13}$
NGC 2264	2×10^{13}
L134	$< 2 \times 10^{13}$
ρOPH	$< 8 \times 10^{12}$
NGC 6334	$< 8 \times 10^{13}$
SGR A	7×10^{14}
SGR B2	2×10^{15}
W33	7×10^{13}
M17L	$< 2 \times 10^{13}$
M17A	3×10^{13}
K39[d]	7×10^{14}
W51	2×10^{14}
B335[e]	$< 4 \times 10^{12}$
DR21(OH)	$< 4 \times 10^{12}$
NGC 7538	3×10^{13}

a. The column densities are derived from measured line strengths and linewidths as given in Table 2. For nondetections the upper limit is obtained from the single channel rms divided by $N^{\frac{1}{2}}$ where N is the number of channels within the FWHM CS linewidth given by Linke and Goldsmith (1980). The kinetic temperature and hydrogen density are taken from Linke and Goldsmith (1980) unless otherwise indicated; b. from Lada et al. 1974; c. from nearby positition discussed by Linke and Goldsmith (1980); d. adopted; e. from Langer et al. 1980).

TABLE 5

OCS FRACTIONAL ABUNDANCE

Source	X(OCS)[a]
ORION A[b]	4×10^{-9}
SGR A	3×10^{-10}
SGR B2	1×10^{-9}
W51	4×10^{-10}

a. Derived using molecular hydrogen density obtained from study of CS (Linke and Goldsmith [illegible], and without inclusion of source-size corrections which are approximately a factor of [illegible] for SgR B2 and 2 for the other sources.

b. The value for Orion A refers to the narrow [illegible] dispersion emission; as discussed in section IVa, the fractional abundance in the high velocity dispersion region is significantly greater.

TABLE 6

$HC^{18}O^+$ OBSERVATIONS, COLUMN DENSITIES, AND COMPARISON WITH OCS

Source	T_A^* (K)	$N(HC^{18}O^+)$ (cm^{-2})	$N(HC^{18}O^+)/N(OCS)$
ORION A	.03	2.5×10^{11}	6×10^{-4}
NGC 2264	.05	3.9×10^{11}	2×10^{-2}
SGR B2	.12	8.2×10^{12}	4×10^{-3}
M17A	.08	8.8×10^{11}	3×10^{-2}
W51	.04	7.9×10^{11}	4×10^{-3}
DR21(OH)	.04	4.0×10^{11}	1×10^{-1}

REFERENCES

Avery, L.W., Oka, T., Broten, N.W., and McLeod, J.M. 1979, Ap. J., 231, 48.

Frerking, M.A., Wilson, R.W., Linke, R.A., and Wannier, P.G. 1980, submitted to Ap. J.

Goldsmith, P.F. 1972, Ap. J., 176, 597.

Goldsmith, P.F. 1977, Bell Sys. Tech. J., 56, 1483.

Goldsmith, P.F., Langer, W.D., Schloerb, F.P., and Scoville, N.Z. 1980, Ap. J., in press.

Green, S., and Chapman, S. 1978, Ap. J. Suppl., 37, 169.

Hartquist, T.W., Oppenheimer, M., and Dalgarno, A. 1980, Ap. J., 236, 182.

Jefferts, K.B., Penzias, A.A., Wilson, R.W., and Solomon, P.M. 1971, Ap. J., 168, L111.

Kuiper, T.B.H., Knapp, G.R., Knapp, S.L., and Brown, R.L. 1976, Ap. J., 204, 408.

Lada, C.J., Gottlieb, C.A., Litvak, M.M., and Lilley, A.E. 1974, Ap. J., 194, 609.

Lada, C.J., Oppenheimer, M.A., and Hartquist, T.W. 1978, Ap. J., 226, L53.

Langer, W.D., Goldsmith, P.F., Carlson, E.R., and Wilson, R.W. 1980, Ap. J., 235, L39.

Lazareff, B., Lucas, R., and Encrenaz, P. 1978, Astron. Astrophys., 70, L77.

Linke, R.A., Schneider, M.V., and Cho, A.Y. 1978, IEEE Trans. Microw. Thy. Tech., MTT-26, 935.

Linke, R.A., and Goldsmith, P.F. 1980, Ap. J., 235, 437.

Maki, A.G. 1974, J. Phys. Chem. Ref. Data, 3, 221.

Morris, M. 1975, Ap. J., 197, 603.

Morris, M., Turner, B.E., Palmer, P., and Zuckerman, B. 1976, Ap. J., 205, 82.

Morris, M., Palmer, P., and Zuckerman, B. 1980, Ap. J., 237, 1.

Oppenheimer, M., and Dalgarno, A. 1974, Ap. J., 187, 231.

Prasad, S.S., and Huntress, W.T. 1980, private communication.

Scoville, N.Z., Solomon, P.M., and Penzias, A.A. 1975, Ap. J., 201, 352.

Solomon, P.M., Jefferts, K.B., Penzias, A.A., and Wilson, R.W. 1971, Ap. J., 168, L107.

Solomon, P.M., Penzias, A.A., Jefferts, K.B., and Wilson, R.W. 1973, Ap. J., 185, L63.

Solomon, P.M., Scoville, N.Z., and Huguenin, G.R. 1980, submitted to Ap. J.

Stark, A.A. 1980, submitted to Ap. J.

Wannier, P.G., and Linke, R.A. 1978, Ap. J., 226, 817.

Winnewisser, G., and Walmsley, C.M. 1978, Astron. Astrophys., 70, L37.

Wootten, A., Evans, N.J. II, Snell, R., and Vanden Bout, P. 1978, Ap. J., 225, L143.

Zuckerman, B., Kuiper, T.B.H., and Kuiper, E.N. 1976, Ap. J., 209, L137.

FIGURE CAPTIONS

Figure 1: OCS J = 7 → 6 spectra in six of the sources we have observed. The abscissa is antenna temperature corrected for antenna beam efficiency. Since the source sizes are found to be comparable to or smaller than the beamsizes used, the peak brightness temperatures will be significantly greater. The line appearing at a velocity ~81 km s^{-1} lower than that of OCS in some of the sources is the J = 1 → 0 transition of $HC^{18}O^{+}$ which has a rest frequency of 85.16216 GHz. The large source to source variation in the relative strengths of these two lines is readily apparent. The noise is lower in a portion of some of the spectra due to the inclusion of data taken as part of a study of $HC^{18}O^{+}$ by Stark 1980.

Figure 2: Excitation curves for OCS under various interstellar conditions. The antenna temperatures for sources filling the beam of an ideal antenna are calculated for different kinetic temperatures; (a) 25 K, (b) 50 K, (c) 75 K. The OCS fractional abundance per unit linewidth is kept fixed.

Figure 3: Spectrum of the J = 11 → 10 transition of OCS in Orion A. The high velocity dispersion emission is clearly visible and has a central velocity of 5 km s^{-1}.

Figure 4: Spectra of OCS transitions in SGR B2.

Figure 5: Spectrum obtained while attempting to detect the J = 7 → 6 transition of OCS in IRC + 10216. The velocity centroid of many lines in this source is -26 km s^{-1}; no OCS emission is detectable at this velocity. We identify the line in the left of the spectrum with the J = 32 → 31 transition of HC_5N.

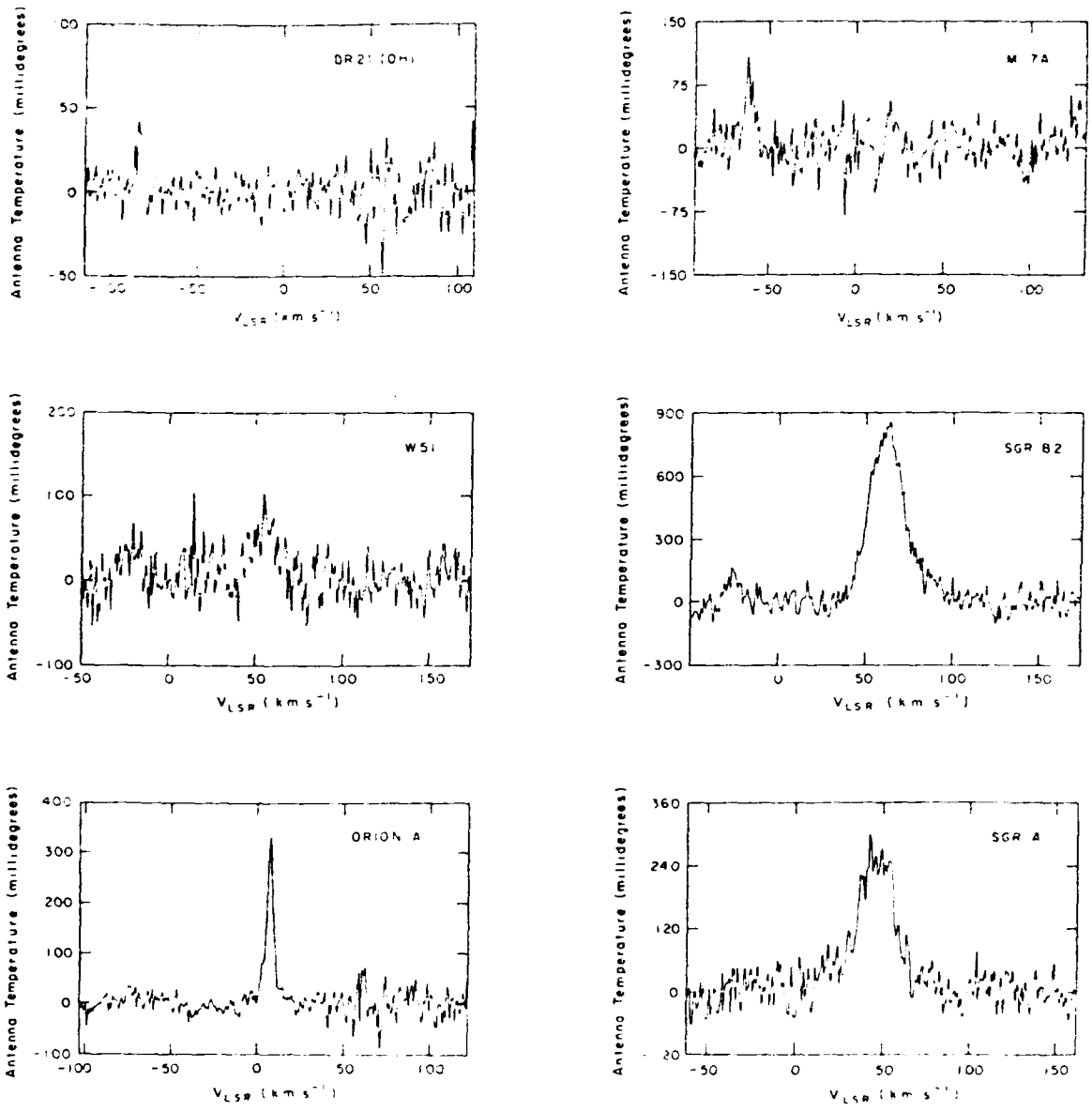
Antenna Temperature (millidegrees)
M 7A
W51
SGR B2
ORION A
SGR A
V_{LSR} (km s^{-1})

FIG 1

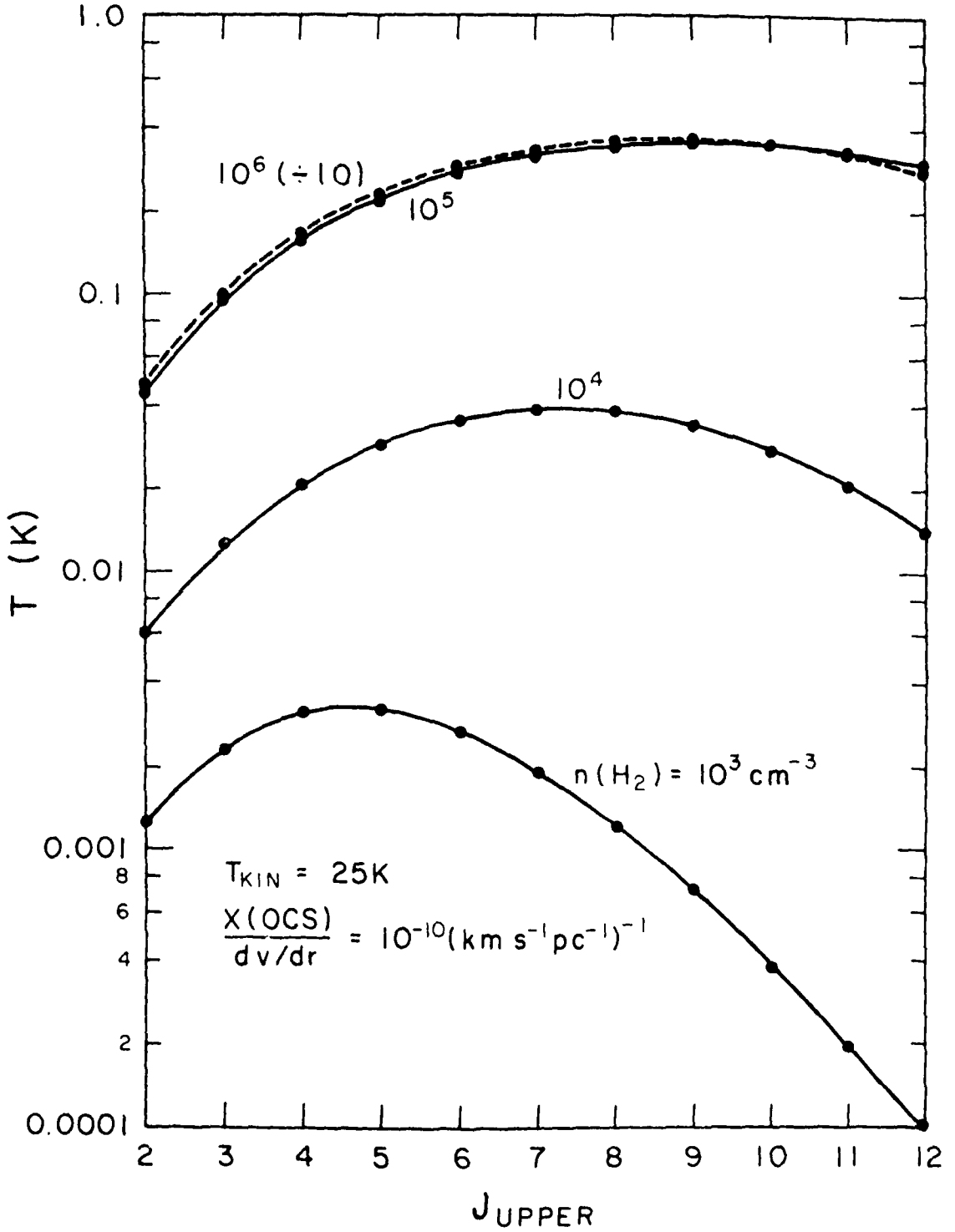
1.0
0.1
0.01
0.001
0.0001
T (K)
8
6
4
2
10^6 (÷10)
10^5
10^4
$n(H_2) = 10^3\ cm^{-3}$
T_{KIN} = 25K
$\frac{X(OCS)}{dv/dr} = 10^{-10}(km\ s^{-1}pc^{-1})^{-1}$
2 3 4 5 6 7 8 9 10 11 12
J_{UPPER}

FIG 2a

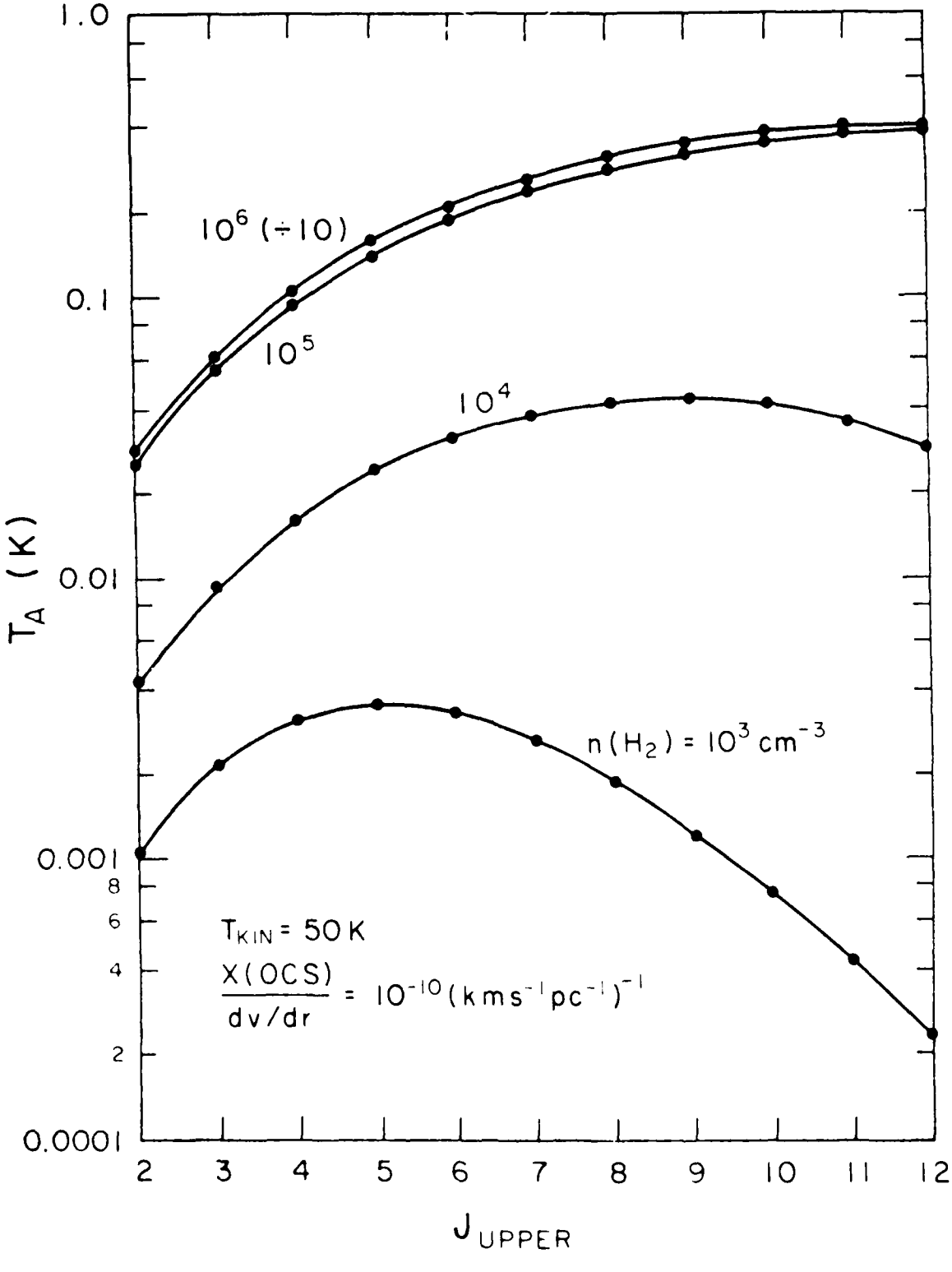
1.0
0.1
0.01
0.001
0.0001
8
6
4
2
T_A (K)
10^6 (÷10)
10^5
10^4
$n(H_2) = 10^3\ cm^{-3}$
$T_{KIN} = 50\ K$
$\frac{X(OCS)}{dv/dr} = 10^{-10}(km\,s^{-1}\,pc^{-1})^{-1}$
2
3
4
5
6
7
8
9
10
11
12
J_{UPPER}

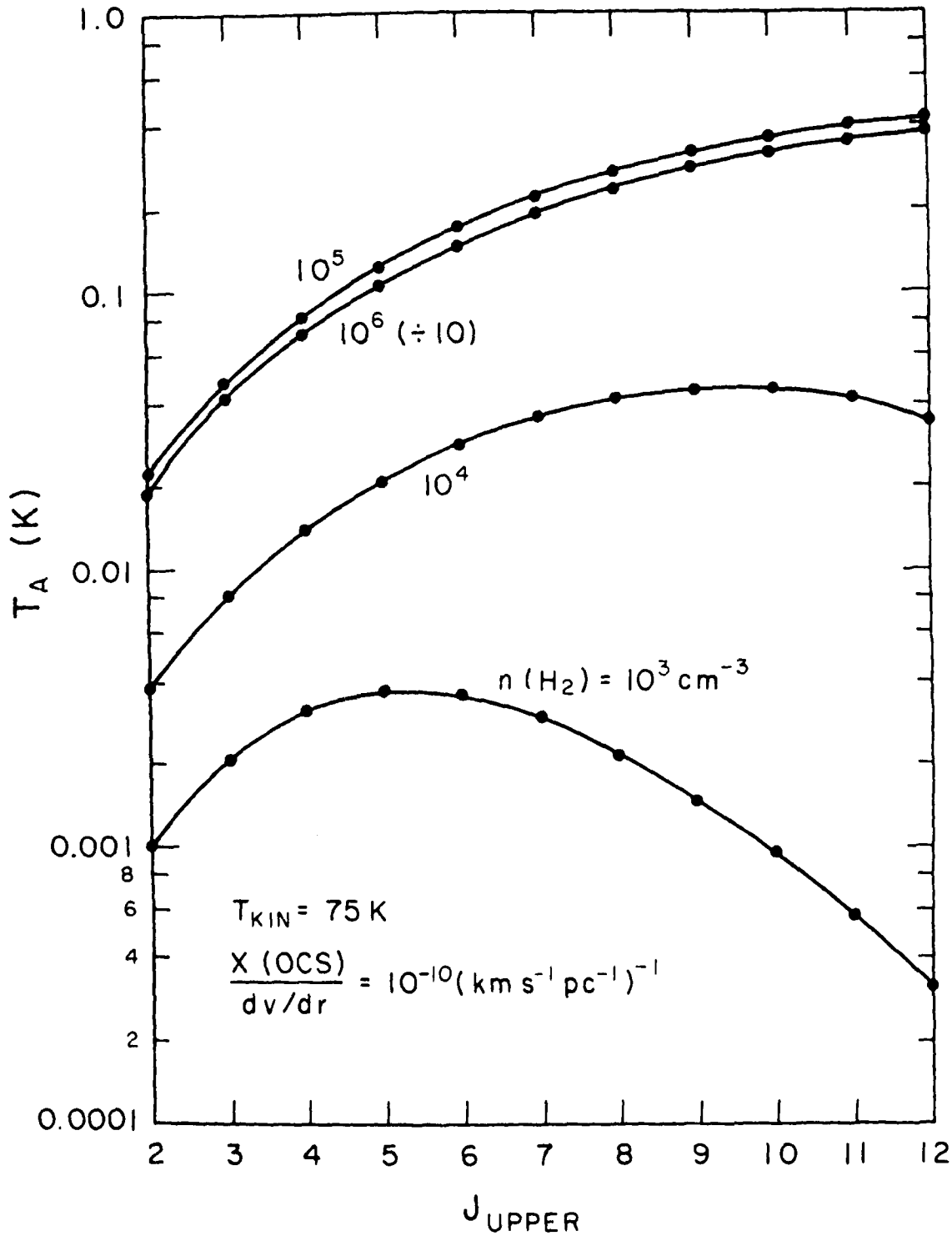
1.0
0.1
0.01
0.001
0.0001
8
6
4
2
T_A (K)
10^5
10^6 (÷10)
10^4
n (H_2) = 10^3 cm^{-3}
T_{KIN} = 75 K
X (OCS) / dv/dr = 10^{-10} (km s^{-1} pc^{-1})$^{-1}$
2 3 4 5 6 7 8 9 10 11 12
J_{UPPER}

FIG 2c

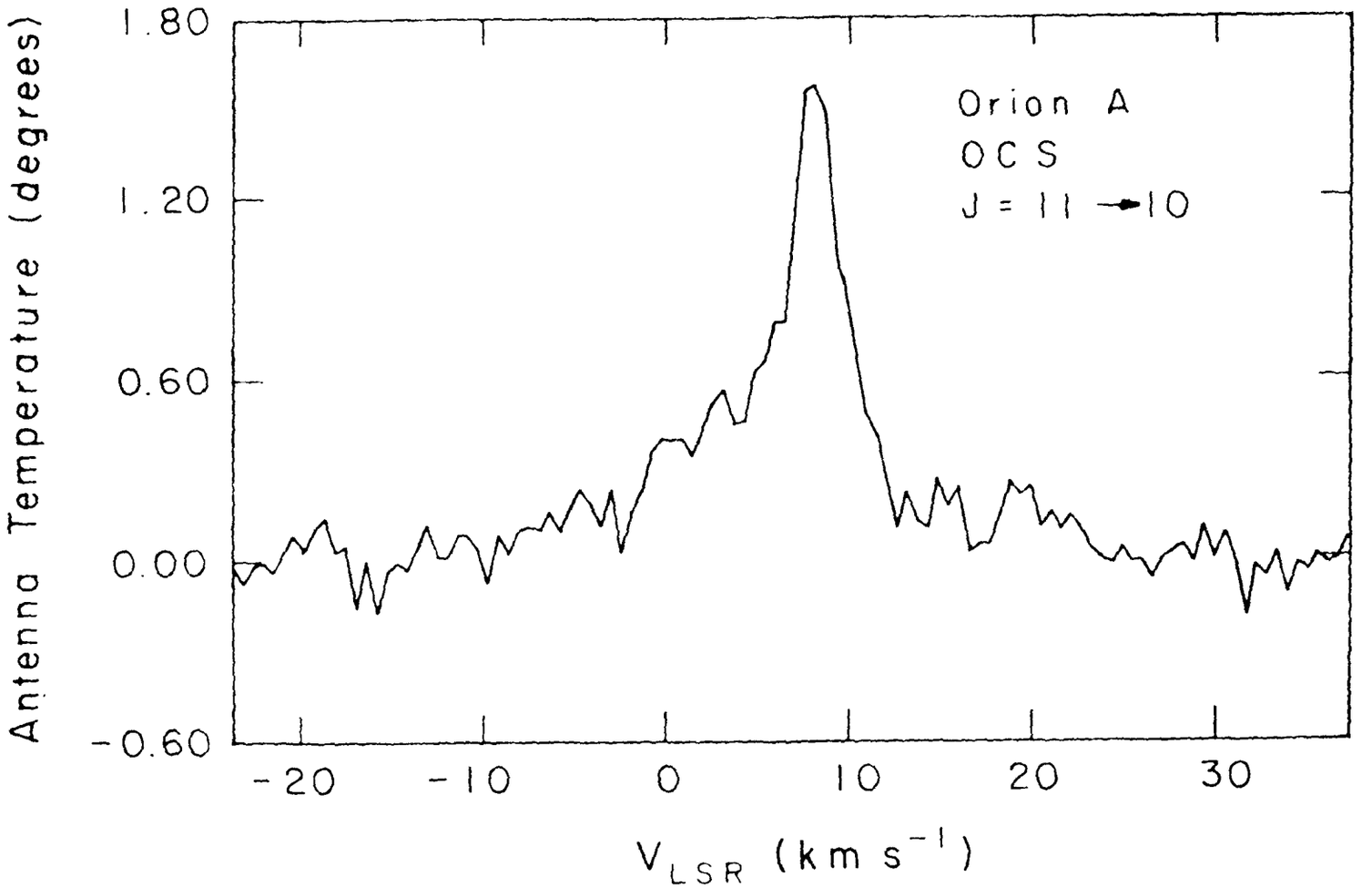
Antenna Temperature (degrees)
1.80
1.20
0.60
0.00
-0.60
-20
-10
0
10
20
30
V_{LSR} (km s^{-1})
Orion A
OCS
J = 11 → 10

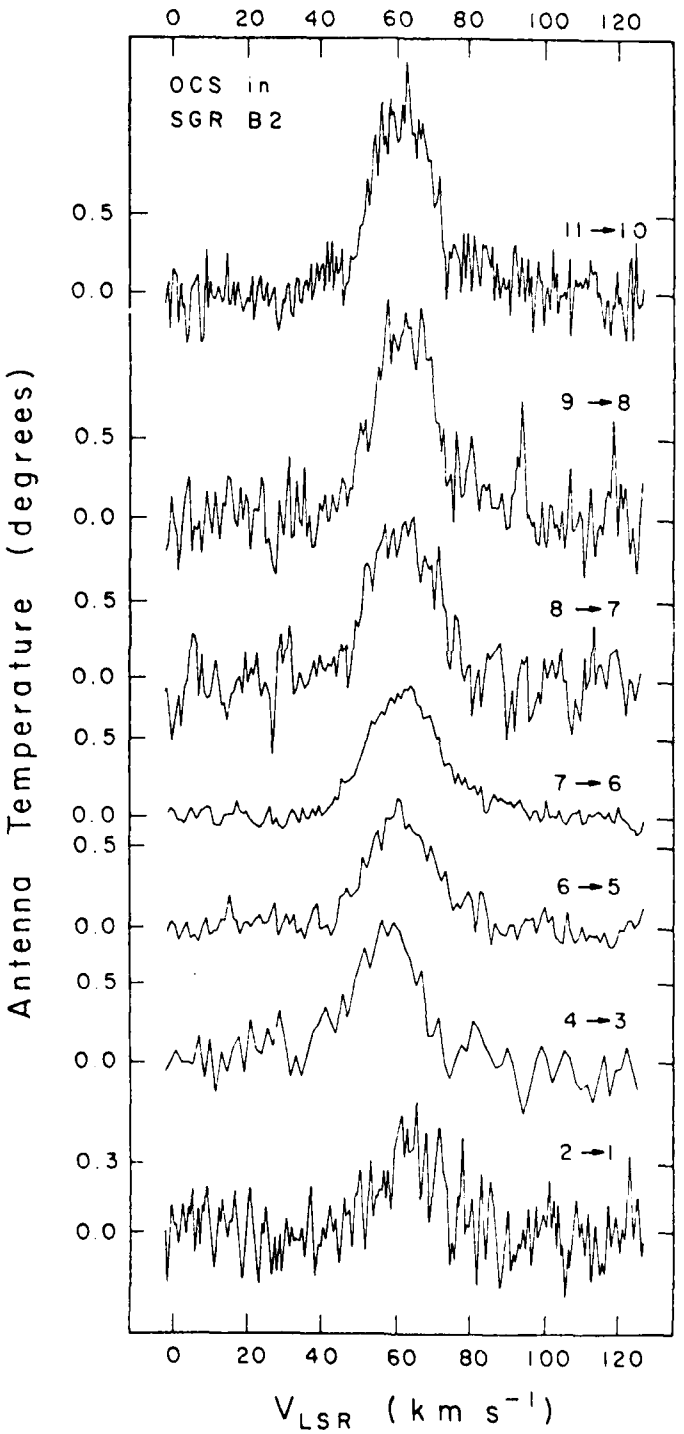
OCS in
SGR B2
11 → 10
9 → 8
8 → 7
7 → 6
6 → 5
4 → 3
2 → 1
0.5
0.0
0.3
0 20 40 60 80 100 120
Antenna Temperature (degrees)
V_{LSR} (km s^{-1})

FIG 4

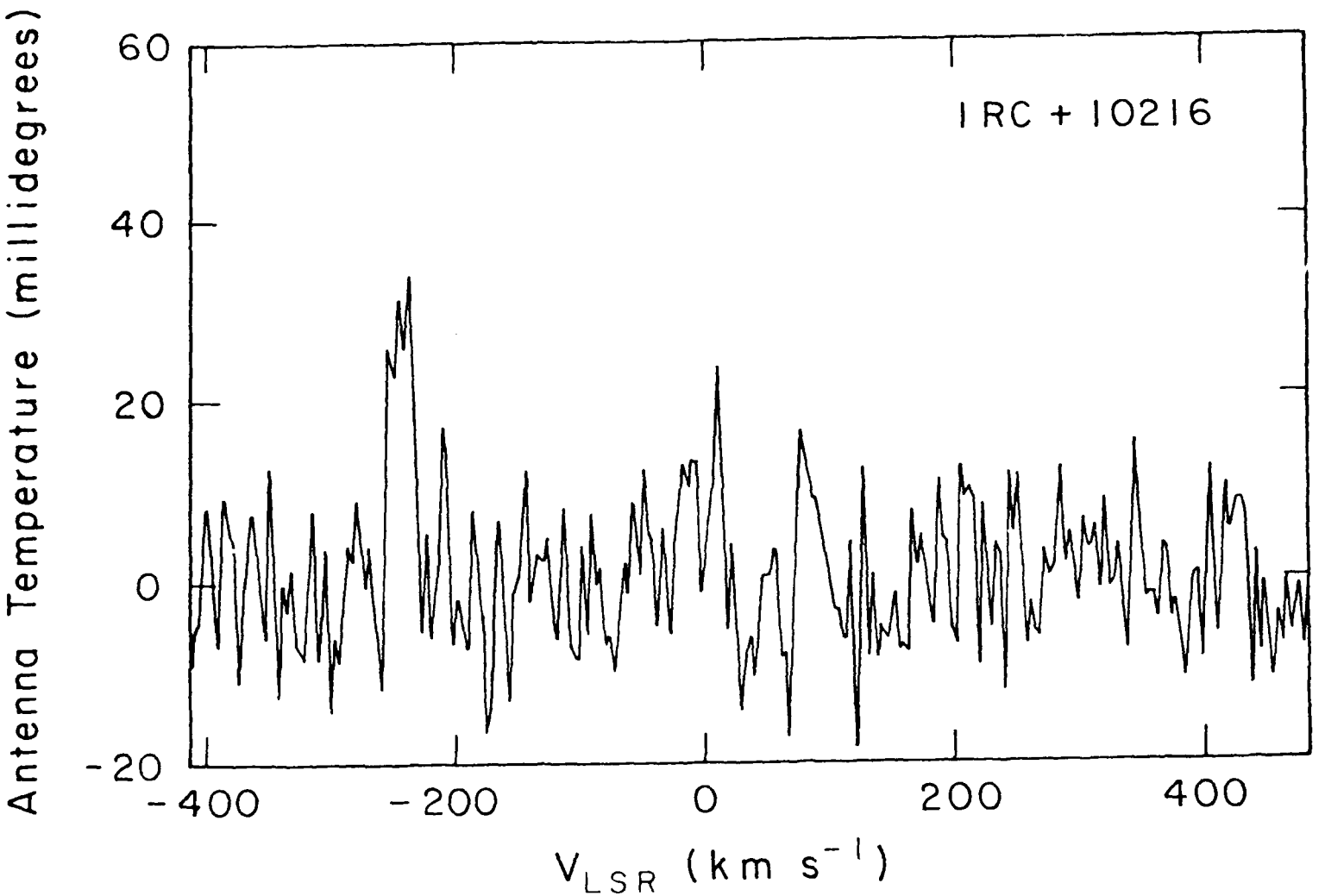
IRC + 10216
Antenna Temperature (millidegrees)
60
40
20
0
-20
-400
-200
0
200
400
V_{LSR} (km s^{-1})

FIG 5

ADDRESSES

Paul F. Goldsmith

Five College Radio Astronomy Observatory

Graduate Research Tower B - Room 626

University of Massachusetts

Amherst, MA 01003

Richard A. Linke

Bell Laboratories

Crawford Hill Laboratory

Holmdel, NJ 07733

END

DATE
FILMED

7-81

DTIC